Eur. Phys. J. D **16**, 245–248 (2001)

THE EUROPEAN PHYSICAL JOURNAL D
EDP Sciences

Formation and stability of large B_6O clusters with icosahedral structure

F. Ding[1,2], G. Wang[1,a] S. Yu[1], J. Wang[1,3], W. Shen[1], and H. Li[1]

[1] National Laboratory of Solid State Microstructures and Department of physics, Nanjing University, Nanjing 210093, P.R. China
[2] Department of Physics, Qufu Normal University, Qufu 273165, P.R. China
[3] Department of Physics, Guangxi University, Nanning 530004, P.R. China

Received 30 November 2000

Abstract. In this paper, the formation and the stability of large B_6O icosahedral particles was discussed on the basis of elastic deformation theory. Our calculation illustrate the stability of macroscopic Mackay packing B_6O icosahedral particles at high pressure. The transition pressure from rhombohedral structure of B_6O particles to macroscopic B_6O icosahedral ones was calculated to be 6 GPa, which is in good agreement with the experimental data (4.0-5.52 GPa). The maximum diameter of B_6O icosahedral particles at low pressure is estimated to be 200–300 nm.

PACS. 61.46.+w Nanoscale materials: clusters, nanoparticles, nanotubes, and nanocrystals – 81.40.Vw Pressure treatment

1 Introduction

Boron suboxide (B_6O or $B_{12}O_2$) is one of the boron-rich compounds [1–3]. The structure of boron-rich compounds are generally based on α-rhombohedral B (α-rh B) and they are characterized by high hardness, low density and chemical inertness [4,5]. Boron suboxide is a kind of superhard material with hardness comparable to that of boron carbide (B_4C) and shows similar abradability of diamond.

In early stages of their formation, many solid materials tend to form icosahedral clusters. However at certain size icosahedral structure become unstable and regular lattice are formed instead [6]. B_6O is an exception where the icosahedral symmetry of Mackay cluster is preserved up to the system with macrospic size.

By sintering the mixture of amorphous B and B_2O_3 in various ratio at high temperature (1700-1800 °C) and high pressure (4.0–5.5 GPa) (HT-HP) [2,3,7], Hubert *et al.* obtained pure and better crystallized B_6O samples with diameter from 1 μm to 40 μm. It is fascinating that these crystals hold an icosahedral structure with five-fold symmetry rather than periodic α-rh B.

Our group have also observed icosahedral particles of B_6O with diameter from 200 nm to 600 nm made by pulsed laser deposition (PLD) method at room pressure [8]. Figure 1 shows the TEM image and the diffraction pattern of a B_6O icosahedral particles aggregate in the nanofilm prepared by PLD method under room pressure.

Figure 2 illustrates a B_2O icosahedron with four layers. When we look at such icosahedral structure from (111)

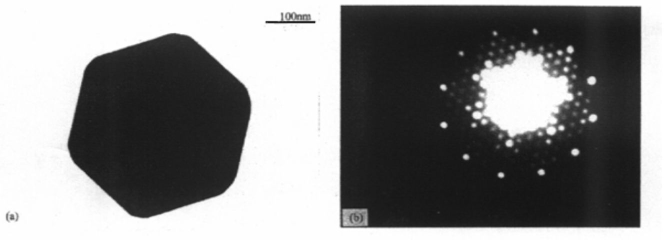

Fig. 1. TEM image (a) and diffraction pattern (b) of a B_6O icosahedral particle aggregate in the nanofilm by PLD under low atmosphere.

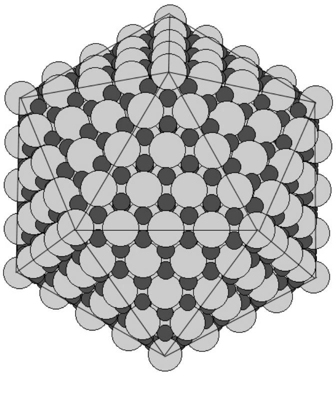

Fig. 2. The structure of a B_6O icosahedron with 4 shells. The small black dots are O atoms and the large circle are B_{12} icosahedra.

---

[a] e-mail: `ghwang@nju.edu.cn`

direction, each B_{12} icosahedron is connected with six O atoms, and each O atom is connected with $3\,B_{12}$ icosahedra in same layer; each B_{12} icosahedron is connected with another $6\,B_{12}$ icosahedra in neighboring layers.

Unlike the self-similar quasicrystal structure of metal alloys [9] and pure single crystals, the B_6O icosahedra are Mackay packing multiply-twined particles (MTPs) [3]. Mackay icosahedral structure is often more stable than periodic structure for small clusters whereas periodic structure will become more stable when cluster size increases. For instance, the number of atoms for rare gas clusters with a structure from icosahedral to periodic is about 1000-2000 (so-called critical number) [10–12]. However, the icosahedral particles of B_6O we obtained by PLD method contain up to 10^{10} atoms, whereas the particles obtained by Hubert *et al.* are composed of up to 10^{14}–10^{16} atoms [2,3,7]. Why can so large Mackay icosahedra be stable? What is the relation between the stability of large B_6O icosahedral particles and the HT-HP environment? In this letter, we will discuss these problems from the view of elastic deformation theory.

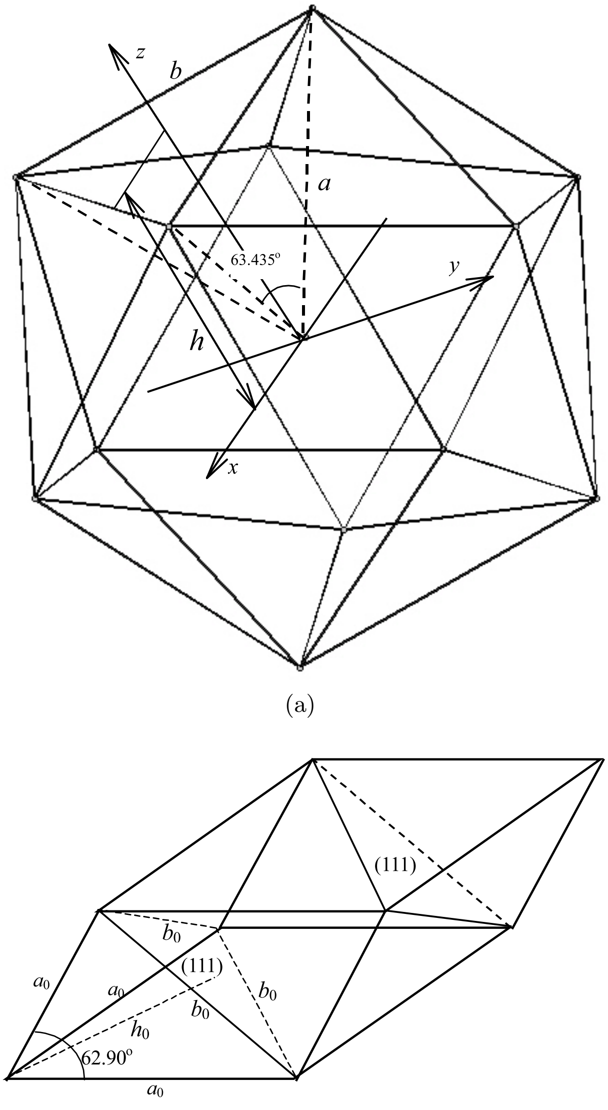

(a)

(b)

Fig. 3. (a) The icosahedral structure and the coordinate system used in this paper, h is the height of the tetrahedron in icosahedron. (b) The structure of B_6O rhombohedral. h_0 is the height of a tetrahedron cut from B_6O rhombohedral by $(1,1,1)$ facet, this tetrahedron will deformed into a tetrahedron in the regular icosahedron as Figure 2 shows.

2 Theory

In fact, a Mackay packing icosahedron can be divided into 20 tetrahedra connected by twin boundaries. These tetrahedra are not regular ones because of the geometrical configuration of icosahedra. The length of the edges on icosahedron surface (b in Figure 3a) are 5.1462% longer than that from the center of the icosahedra to the vertices (a in Figure 3a), and the angle between two neighboring edges from the center to vertices is $\theta_{ico} = 63.435$ degree whereas $\theta_0 = 60.00$ degree for a regular tetrahedron. This means that these tetrahedra must be deformed in order to form a regular icosahedron, and thus elastic energy exists in the icosahedron.

It is well known that the stability of Mackay packing icosahedral particles comes from the lower surface energy whereas the elastic energy contributes to the instability of the icosahedra [13]. For large clusters contains N atoms, we can suggest that the surface energy difference between an icosahedron and corresponding periodic structure is $\Delta E_s = \varepsilon_s N^{2/3}$ (ε_s is a constant), and the elastic energy of the icosahedron is $E_{el} = \varepsilon_{el} N$ (ε_{el} is the average elastic energy density in icosahedral particles). When $\Delta E_s = E_{el}$, the critical number can be described by:

$$N_c \propto \left(\frac{\varepsilon_s}{\varepsilon_{el}}\right)^3. \tag{1}$$

Eq. (1) indicates that the critical number is inversely proportional to the cube of the elastic energy density ε_{el}. For an icosahedral cluster with corresponding bulk material of fcc structure, the angle deformation is $\Delta\theta_{fcc} = 3.435$ degree, whereas the angle deformation of B_6O rhombohedral crystal is $\Delta\theta_{\mathrm{B_6O}} = 0.535$ degree. $\Delta\theta_{\mathrm{B_6O}}$ is only one seventh of $\Delta\theta_{fcc}$ because the angle $\alpha = 62.90$ degree of B_6O rhombohedral crystal (in Figure 3b) is much similar to $\theta_{\mathrm{ico}} = 63.435$ degree [14–16]. Hubert *et al.* have proposed that the similarity of the two angles may contribute to the stability of large B_6O icosahedra. We can expand the elastic energy ε_{el} to the second order of the angle deformation $\Delta\theta$, and estimate that the critical number of B_6O is

$$N_{c\mathrm{B_6O}} = \left(\frac{\Delta\theta_{fcc}}{\Delta\theta_{\mathrm{B_6O}}}\right)^6 N_{cfcc} = 7\times10^4 N_{cfcc}, \tag{2}$$

where N_{cfcc} is the critical number of icosahedral clusters with fcc structure of corresponding bulk material and $N_{c\mathrm{B_6O}}$ is the critical number of B_6O icosahedral particles. Although N_{cfcc} is material dependent, its value ranges from hundreds to several thousands of atoms for most materials [17]. Therefore, we can obtain that the order of N_{cB_6O} is 10^7–10^8 with diameter about 200–300 nm, similar to that obtained by our group in PLD experiments (200–600 nm) shown in Figure 1a. This estimation is effective only for low pressure since the external pressure is not considered.

At high pressure, the size of B_6O icosahedral particles up to 40 μm [2,3,7]. For so large B_6O particles with number of atoms N up to 10^{15}–10^{16}, the surface energy should be much smaller than the elastic energy at high pressure since the surface energy is proportional to $N^{2/3}$ whereas the elastic energy is proportional to N. Therefore, the stability of a structure may depend on its elastic energy only at high pressure.

Now let's perform a detailed calculation of the elastic deformation and elastic energy in icosahedral B_6O particles. Considering a tetrahedron in the icosahedron as shown in Figure 3a, we prefer to make some suggestions to simplify the problem first.

1. The elastic deformation and the elastic tension only depend on the coordinate z because of the layer structure of icosahedron and the boundary condition on the surface.
2. Both the shear deformation and the shear tension at all surfaces of the tetrahedron are zero because of the symmetry and the boundary condition. Thus, it is reasonable to neglect the shear components of the elastic deformation and the elastic tension.

Then we can denoting $e_{xx}(z) = e_{yy}(z)$, $\sigma_{xx}(z) = \sigma_{yy}(z)$, $e_{zz}(z)$ and $\sigma_{zz}(z)$ as the elastic deformation and elastic tension components in x–y plane and those along z-direction.

The tetrahedron in the icosahedron is deformed by a tetrahedron cut from B_6O rhombohedron by the $(1,1,1)$ facet (Figure 3b). The length of edges on $(1,1,1)$ facet is deformed from b_0 to $b = (1 + e_{xx}(z))b_0$, the height is deformed from h_0 to $h = \left(1 + \frac{1}{z}\int_0^z e_{zz}(\xi)\,d\xi\right) h_0$. The ratio of b and h should be $\frac{b}{h} = \frac{1}{\sqrt{\left(\frac{1}{1+0.051462}\right)^2 - \frac{1}{3}}}$. This relation should hold for any small tetrahedron from center to z because the small tetrahedron from center to z is one part of a small icosahedron. Thus, we have a constraint equation:

$$\frac{1 + e_{xx}(z)}{1 + \frac{1}{z}\int_0^z e_{zz}(\xi)\,d\xi} = 1 + \delta, \qquad z \in [0, h], \tag{3}$$

where $\delta = 0.01203$ for B_6O and h is the height of the tetrahedron. Assuming P_0 as the external pressure under which B_6O icosahedra grows, the boundary condition at the surface can be written as:

$$\sigma_{zz}(h) = -P_0. \tag{4}$$

3. The elastic tension at three surfaces in the icosahedron is supposed to be the same as $\sigma_{xx}(z)$. The total external force on any part in the tetrahedron from $z - z + dz$ should be zero. Thus we can obtain another equation

$$\sigma_{xx}(z) = \sigma_{zz}(z) + \frac{1}{2} z \frac{d\sigma_{zz}(z)}{dz} \qquad z \in [0, h]. \tag{5}$$

Without considering the shear components of stress tensor and deformation tensor, the Hooke's law is:

$$\begin{pmatrix} \sigma_{xx}(z) \\ \sigma_{xx}(z) \\ \sigma_{zz}(z) \end{pmatrix} = \begin{pmatrix} C_{11} & C_{12} & C_{13} \\ C_{12} & C_{11} & C_{13} \\ C_{13} & C_{13} & C_{33} \end{pmatrix} \begin{pmatrix} e_{xx}(z) \\ e_{xx}(z) \\ e_{zz}(z) \end{pmatrix}. \tag{6}$$

where $C_{11} = 5.8688 \times 10^{11}$ Pa, $C_{12} = 1.3319 \times 10^{11}$ Pa, $C_{13} = 0.4741 \times 10^{11}$ Pa, $C_{33} = 4.4385 \times 10^{11}$ Pa are the elastic modulus of B_6O rhombohedra [14]. The above formula can be simply rewritten as:

$$\begin{pmatrix} e_{xx}(z) \\ e_{zz}(z) \end{pmatrix} = \begin{pmatrix} A_{11} & A_{12} \\ A_{21} & A_{22} \end{pmatrix} \begin{pmatrix} \sigma_{xx}(z) \\ \sigma_{zz}(z) \end{pmatrix}, \tag{7}$$

where $A_{11} = \frac{1}{\Delta} C_{33}$, $A_{12} = -\frac{1}{\Delta} C_{13}$, $A_{21} = -\frac{2}{\Delta} C_{13}$, $A_{22} = \frac{1}{\Delta}(C_{11} + C_{12})$, $\Delta = C_{11}C_{33} + C_{33}C_{12} - 2C_{13}^2$.

Introducing Eq. (5) and Eq. (7) to constraint equation (3), we can have an Euler's differential equation,

$$\alpha\zeta^2 \frac{d^2\sigma_{zz}(\zeta)}{d\zeta^2} + (2\alpha + \beta)\,\zeta \frac{d\sigma_{zz}(\zeta)}{d\zeta} + (\beta + \gamma)\,\sigma_{zz}(\zeta) - \delta = 0, \tag{8}$$

where $\zeta = \frac{z}{h}$, $\alpha = 0.5A_{11}$, $\beta = A_{11} + A_{12} - 0.5(1 + \delta)A_{21}$, $\gamma = -(1 + \delta)(0.5A_{21} + A_{22})$. Eq. (8) can be solved analytically with the boundary condition (4). The expressions of elastic tension σ_{xx}, σ_{zz} are obtained as follows

$$\begin{aligned} \sigma_{xx}(\zeta) &= -P_T + (P_T - P_0)(1 + 0.5n)\zeta^n, \\ \sigma_{zz}(\zeta) &= -P_T + (P_T - P_0)\zeta^n, \end{aligned} \tag{9}$$

where $P_T = \frac{\delta\Delta}{\{(1+\delta)(C_{11}+C_{12}) - C_{33} - (1+2\delta)C_{13}\}}$, $n = \frac{1}{2\alpha}[-(\alpha + \beta) + \sqrt{(\alpha + \beta)^2 - 4\alpha(\beta + \gamma)}]$, (another solution $n = \frac{1}{2\alpha}[-(\alpha + \beta) - \sqrt{(\alpha + \beta)^2 - 4\alpha(\beta + \gamma)}] < 0$ was rejected because of the natural boundary condition: $\sigma_{zz}(z = 0)$ should be finite). We introduce above formula into Eq. (7) and have the elastic deformation e_{xx} and e_{zz},

$$\begin{aligned} e_{xx}(\zeta) &= D_{11}\zeta^n + D_{12}, \\ e_{zz}(\zeta) &= D_{22}\zeta^n + D_{21}, \end{aligned} \tag{10}$$

where$D_{11} = (P_T - P_0)\,[A_{11}(1 + 0.5n) + A_{12}]$, $D_{12} = -P_T(A_{11} + A_{12})$, $D_{21} = -P_T(A_{21} + A_{22})$, $D_{22} = (P_T - P_0)\,[A_{21}(1 + 0.5n) + A_{22}]$ are constants. The elastic energy density distribution ε_{ico} and average elastic energy density $\overline{\varepsilon_{ico}}$ in the icosahedron are

$$\begin{aligned} \varepsilon_{ico}(\zeta) &= D_2\zeta^{2n} + D_1\zeta^n + D_0, \\ \overline{\varepsilon_{ico}} &= D_0 + \frac{3D_1}{n + 3} + \frac{3D_2}{2n + 3}, \end{aligned} \tag{11}$$

where $D_2 = (P_T - P_0)\,[D_{11}(1 + 0.5n) + 0.5D_{22}]$, $D_1 = (P_T - P_0)\,[D_{12}(1 + 0.5n) + 0.5D_{21}] - P_T\,(D_{11} + 0.5D_{22})$, $D_0 = P_T^2(A_{11} + A_{12} + 0.5A_{21} + 0.5A_{22})$.

From above we have obtained the elastic energy density in B_6O icosahedral particles under pressure P_0. For B_6O periodic structure the elastic energy density under the external pressure P_0 can be described as:

$$\overline{\varepsilon_1}(P_0) = (A_{11} + A_{12} + 0.5A_{21} + 0.5A_{22})P_0^2. \tag{12}$$

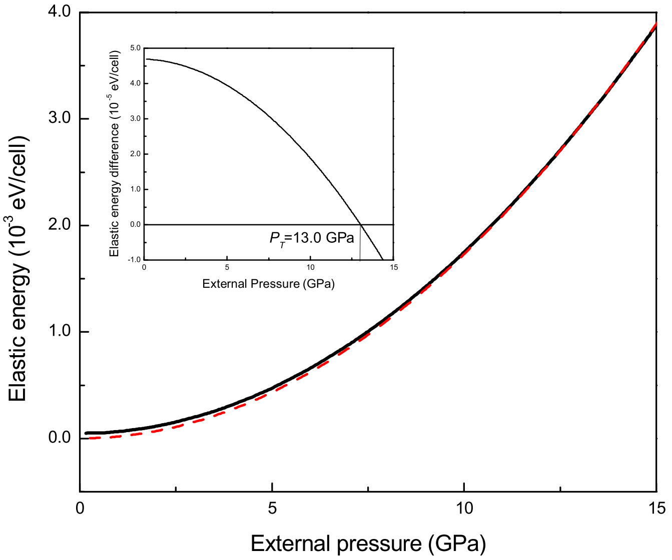

Fig. 4. The external pressure dependence average elastic energy density for B_6O icosahedron (solid line) and B_6O periodic structure (dash line). The inserted figure shows the elastic energy density difference between B_6O periodic structure and B_6O icosahedron.

3 Discussion

Figure 4 shows the external pressure dependence of average energy density for the B_6O icosahedra and B_6O periodic structure. It clearly shows that $\overline{\varepsilon_{ico}} > \overline{\varepsilon_1}$ when $P_0 < P_T$ and $\overline{\varepsilon_{ico}} < \overline{\varepsilon_1}$ when $P_0 > P_T$. That indicates B_6O icosahedral particles at large size are more stable than rhombohedral structure at high pressure $P_0 > P_T$ whereas the rhombohedral structure is more stable at low pressure $P_0 < P_T$. Here $P_T = 13.0$ GPa is the transition pressure for B_6O from the rhombohedral structure to the macroscopic icosahedral structure.

Hubert *et al.* obtained B_6O icosahedral particles with size up to 40 μm [2,3,7]. The external pressure in their experiments is about 4−5.5 GPa, about 2−3 times lower than the transition pressure $P_T = 13.0$ GPa obtained in the present calculation. However, we have not taken into account of the temperature effects. In fact, elastic modulus of material will decrease with increasing temperature [18,19]. According to the results of Tushishvili *et al.* [18], the elastic modulus of B_6O can be expected to decrease more than 20% at the temperature of 1700-1800 °C. Another possible reason is that the expansion rate of B_6O rhombohedral crystals in z-direction may be different from that in $x-y$ plane because of the anisotropic of the B_6O rhombohedral crystal. Therefore the angle α may change with temperature. Very small amount of increase for angle α will lead to a significant decrease of $\Delta\theta_{B_6O}$ and the transition pressure P_T. There we have two different experimental values of angle α, 63.1 degree given Hubert *et al.* in their papers [2,3,7] and 62.90 by others [14–16]. If we suggest that the modulus at high temperature be reduced by 20% and $\alpha =$ 63.1 degree, the transition pressure will be about 6 GPa, which is in good agreement with the external pressure used by Hubert *et al.* [2,3,7].

In conclusion, we have discussed the stability of macroscopic B_6O icosahedral particles at high pressure. The maximum diameter of stable B_6O icosahedral particles at low pressure are estimated to be in good agreement with our experimental results.

This work performed under the auspices of National Nature Foundation of China (No. 29890210) and Nature Science Foundation of Shandong China (No. Q99A04).

References

1. C.L. Beckel, M. Yousaf, M.Z. Fuka, S.Y. Raja, N. Lu, Phys. Rev. B **44**, 2535 (1991).
2. H. Hubert, L.A.J. Garvie, B. Devouard, P.R. Buseck, W.T. Petuskey, P.F. McMillan, Chem. Mater. **10**, 1530 (1998).
3. H. Hubert, B. Devouard, L.A.J. Garvie, M. O'Keeffe, P.R. Buseck, W.T. Petuskey, P.F. McMollan, Nature **391**, 376 (1998).
4. A.R. Badzian, Appl. Phys. Lett. **53**, 2495 (1988).
5. H. Ioh, I. Maekawa, H. Iwahara, J. Mater. Sci. **35**, 693 (2000)
6. P.K. Doye, D.J. Wale, J. Chem. Soc., Faraday Trans. **93**, 4233 (1997).
7. P.F. McMillan *et al.*, J. Solid. Chem. **147**, 281 (1999).
8. S.W. Yu *et al.*, Phys. Lett. A. **268**, 442 (2000).
9. D. Shechtman, I. Blech, D. Gratias, J.W. Cahn, Phys. Rev. Lett. **53**, 1951 (1984).
10. B.W. van der Waal, J. Chem. Phys. **90**, 3407 (1989).
11. B.W. van der Waal, J. Chem. Phys. **98**, 4909 (1993).
12. B.W. van der Waal, Phys. Rev. Lett. **76**, 1083 (1996).
13. S. Ino, J. Phys. Soc. Jap. **27**, 941 (1969).
14. S. Lee, D.M. Bylander, L. Kleinman, Phys. Rev. B **45**, 3245 (1992).
15. S. Lee, S.W. Kim, D.M. Bylander, L. Kleinman, Phys. Rev. B **44**, 3550 (1991).
16. I. Higashi, M. Kobayashi, J. Bernhard, C. Brodhag, F. Therenot, in *Tenth International Symposium on Boron, Borides and Related Compounds*, Albuquerque, NM (AIP, New York, 1990).
17. P.A. Montano, W. Schulze, B. Tesche, G.K. Shenoy, T.L. Morrison, Phys. Rev. B. **30**, 6292 (1984).
18. M.Ch. Tushishvili, G.V. Tsagareishvili, D.Sh. Tsagareishvili, J. Hard Mater. **3**, 225 (1992).
19. F. Szuecs, M. Werner, R.S. Sussmann, C.S.J. Pickles, H.J. Fecht, J. Appl. Phys. **86**, 6010 (1999).